

# Terahertz Conductivity at the Verwey Transition in Magnetite

A. Pimenov, S. Tachos, T. Rudolf, and A. Loidl

*Experimentalphysik V, EKM, Universität Augsburg, 86135 Augsburg, Germany*

D. Schrupp, M. Sing, and R. Claessen

*Experimentalphysik II, Universität Augsburg, 86135 Augsburg, Germany*

V. A. M. Brabers

*Department of Physics, Eindhoven University of Technology, NL-5600, MB Eindhoven, The Netherlands*

(Dated: October 2, 2018)

The complex conductivity at the (Verwey) metal-insulator transition in  $\text{Fe}_3\text{O}_4$  has been investigated at THz and infrared frequencies. In the insulating state, both the dynamic conductivity and the dielectric constant reveal a power-law frequency dependence, the characteristic feature of hopping conduction of localized charge carriers. The hopping process is limited to low frequencies only, and a cutoff frequency  $\nu_1 \simeq 8 \text{ meV}$  must be introduced for a self-consistent description. On heating through the Verwey transition the low-frequency dielectric constant abruptly decreases and becomes negative. Together with the conductivity spectra this indicates a formation of a narrow Drude-peak with a characteristic scattering rate of about  $5 \text{ meV}$  containing only a small fraction of the available charge carriers. The spectra can be explained assuming the transformation of the spectral weight from the hopping process to the free-carrier conductivity. These results support an interpretation of Verwey transition in magnetite as an insulator-semiconductor transition with structure-induced changes in activation energy.

## I. INTRODUCTION

Magnetite ( $\text{Fe}_3\text{O}_4$ ) is probably the oldest known magnetic material, which can be found in natural form. This material is of considerable importance because of various applications in magnetic recording and for high-frequency electronic devices. Physical properties of magnetite have attracted much attention after the discovery of the first-order metal-insulator transition at  $T_V \sim 120 \text{ K}$ . On cooling through the transition temperature the dc-conductivity drops by two orders of magnitude. A realistic model to explain the mechanism of this transition has been suggested by Verwey [1], assuming a charge order-disorder transition with alternating valence ( $\text{Fe}^{2+}/\text{Fe}^{3+}$ ) of the octahedrally-coordinated iron ions. The metal-to-insulator transition in magnetite has been termed Verwey transition since then. In spite of a large number of experimental and theoretical efforts, the mechanism governing the conduction and magnetic properties in magnetite is still under debate [2, 3]. According to the results of recent x-ray resonant scattering [4], even the charge-ordering below  $T_V$  has been questioned and the concept of an itinerant magnet was considered instead. Also the importance of the orbital degrees of freedom have recently been highlighted [5].

Magnetite crystallizes in a cubic high-temperature structure and exhibits a monoclinic distortion below the Verwey transition. In spite of enormous progress in resolving the low-temperature monoclinic structure of magnetite [6, 7, 8], full details could not be completely resolved so far. The monoclinic phase is insulating and is characterized by a gap of the order of  $100 \text{ meV}$  in the excitation spectrum, which is seen in photoemission data [9, 10, 11], in thermoelectric properties [12], and by

optical spectroscopy [13, 14]. The charge transport in magnetite is usually explained within a polaronic picture [13, 14, 15, 16]. However, there is no general agreement about the energy of the polaronic absorption in the conductivity spectra [13, 14, 15, 16]. Recent photoemission results [11], obtained in the same magnetite crystals as in the present work, have been self-consistently explained using a small-polaron model. A similar concept has been applied recently to explain the dynamic conductivity at the metal-insulator transition in quasi-one-dimensional  $\beta\text{-Na}_{0.33}\text{V}_2\text{O}_5$  [17].

At low-temperatures the conduction in magnetite takes place via hopping between localized states, which agrees well with both activated dc-resistivity [18, 19, 20] and with an observed characteristic power-law  $\sigma \propto \nu^s$  [21] of the ac-conductivity. This universal [22] power-law has been observed in various materials with internal disorder and is a clear fingerprint of hopping of charge carriers [23, 24, 25]. The situation is getting more complicated in the metallic state. In spite of two orders-of-magnitude increase in resistance above  $T_V$ , the absolute value of the dc-conductivity ( $\sigma_{dc}(T \gtrsim T_V) \sim 50 \Omega^{-1}\text{cm}^{-1}$ ) is still much smaller than the Ioffe-Regel [26] minimum metallic conductivity  $\sigma_{min} \sim e^2/3\hbar a \sim 3000 \Omega^{-1}\text{cm}^{-1}$ , even including the Mott correction [27] in case of disorder  $\sigma_{min} \sim 0.03e^2/\hbar a \sim 300 \Omega^{-1}\text{cm}^{-1}$  (here  $a \sim 3 \text{ \AA}$  is the interatomic distance). The high-temperature conductivity of magnetite is thus typical for a semiconductor with a high mobility of thermally-excited charge carriers rather than for a metal. Reviews of the recent and past developments in magnetite can be found in [2, 3, 28, 29, 30].

In this paper we investigate Terahertz and infrared conductivity of magnetite on both sides of the metal-to-insulator transition. The unexpected result of these ex-

periments is the abrupt change of the dielectric constant at the transition temperature yielding even negative values above  $T_V$ . Together with the conductivity spectra these results indicate the formation of a narrow band of quasi-free carriers which contains only a small part of the total spectral weight.

## II. EXPERIMENTAL DETAILS

Synthetic single crystals of magnetite were prepared from  $\alpha\text{-Fe}_2\text{O}_3$  (spec. pure) using a floating-zone method with radiation heating [31]. Two single crystals were used for the measurements, which revealed slightly different transition temperatures,  $T_V \simeq 123 \pm 1$  K and  $116 \pm 1$  K, respectively. The transition temperature in magnetite can be taken as a criterium for impurity concentration and oxygen stoichiometry [2, 32] which, therefore, differ significantly for the two crystals investigated. Both samples revealed qualitatively similar electrodynamic properties revealing only differences in absolute values. Therefore, in the following mainly the results on a sample with  $T_V \simeq 123$  K will be shown. Plane-parallel samples of different thickness between 0.5 mm and 0.05 mm have been prepared from the original boules. To ensure mechanical stability, the thinnest samples were glued onto a MgO substrate of  $\simeq 0.5$  mm thickness. The availability of samples with different thicknesses is essential for transmittance experiments due to the strongly temperature-dependent absorption in magnetite.

The dynamic experiments for frequencies  $4 \text{ cm}^{-1} < \nu < 40 \text{ cm}^{-1}$  were carried out in a Mach-Zehnder interferometer arrangement [33] which allows both, the measurements of the transmittance and the phase shift of a plane-parallel sample. The complex transmission coefficient has been analyzed using the Fresnel optical formulas for transmittance  $T = |t|^2$  of a plane-parallel sample [34, 35]:

$$t = \sqrt{T} e^{i\phi_T} = \frac{(1 - r^2)t_1}{1 - r^2 t_1^2}, \quad (1)$$

$$\text{where } r = \frac{\sqrt{\varepsilon} - 1}{\sqrt{\varepsilon} + 1} \text{ and } t_1 = \exp(-2\pi i \sqrt{\varepsilon} d/\lambda).$$

Here  $r$  is the reflection amplitude of a thick sample,  $t_1$  is the “pure” transmission amplitude,  $\varepsilon$  is the complex dielectric permittivity of the sample,  $d$  is the sample thickness, and  $\lambda$  is the radiation wavelength. It has been assumed that the magnetic permeability  $\mu = 1$  in the frequency range of our experiments. The transmittance for a two-layer system can be obtained in a similar way [34, 35]. Using Eq. (1) the absolute values of the complex conductivity  $\sigma^* = \sigma_1 + i\sigma_2$  and dielectric constant  $\varepsilon^* = \varepsilon_1 + i\varepsilon_2 = \sigma^*/i\varepsilon_0\omega$  can be determined directly from the measured spectra. Here  $\varepsilon_0$  and  $\omega = 2\pi\nu$  are the permittivity of vacuum and the angular frequency, respectively. In general, the phase shift  $\phi_T$  in the transmittance experiment contains a possible ambiguity of  $2\pi \cdot n$ , where

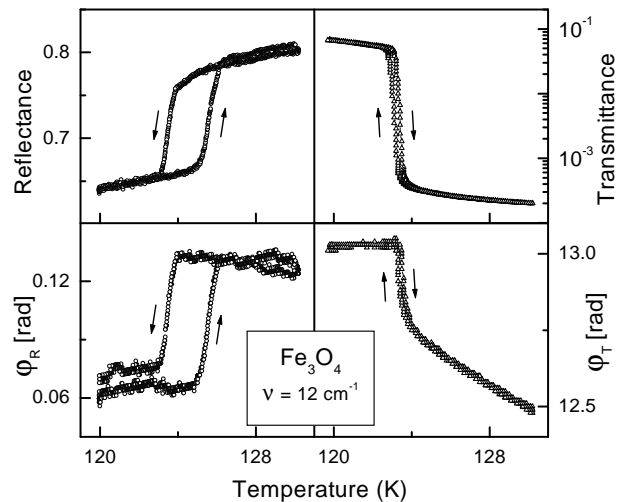


FIG. 1: Left panels: temperature-dependent reflectance (top left) and reflectance phase-shift (bottom left) of magnetite at  $\nu = 12 \text{ cm}^{-1}$  in the vicinity of the Verwey transition. Right panels: transmittance (top) and phase shift (bottom) of a 0.05 mm thick plane-parallel sample glued on the 0.5 mm thick MgO substrate. The four measured quantities represent two data-sets to determine  $\sigma_1$  and  $\varepsilon_1 = -\sigma_2/\varepsilon_0\omega$ .

$n$  is an integer. To exclude this source of errors, the reflectance of thick sample has been measured in addition to transmittance experiments. A similar Mach-Zehnder arrangement allowed to obtain the amplitude and the phase shift of the reflectance at the Verwey transition. In total, a set of four measured quantities was available to calculate the real and imaginary part of the dynamic conductivity in the THz frequency range.

In the infrared and visible frequency ranges  $30 \text{ cm}^{-1} < \nu < 21000 \text{ cm}^{-1}$  the complex conductivity has been obtained via the Kramers-Kronig analysis of the reflectivity of the thick sample. The reflectivity experiment were performed using Bruker IFS-113v and IFS 66v/S Fourier-transform spectrometers. Different sources, beam splitters and optical windows allowed to cover the complete frequency range. In addition, the reflectance for the frequency range  $4 < \nu < 40 \text{ cm}^{-1}$  has been calculated using the complex conductivity data, obtained by the transmittance technique, described above. The combination of the results from two experimental techniques [36] substantially expands the low-frequency limit of the available spectrum and the quality of the subsequent Kramers-Kronig transformation.

## III. RESULTS AND DISCUSSION

Figure 1 shows the complex reflectance and transmittance of magnetite in the vicinity of Verwey transition. All four quantities reveal strong changes at the transition temperature. The most dramatic changes are observed in the transmittance, that decreases by

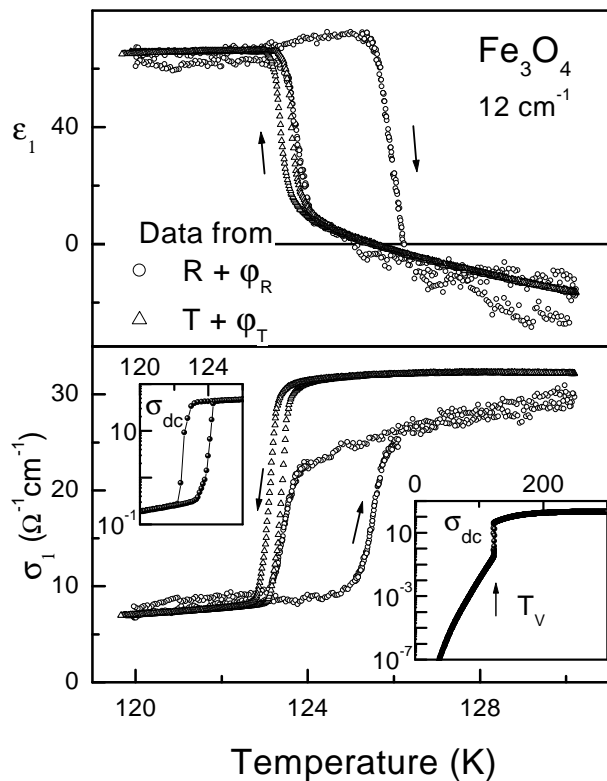


FIG. 2: Temperature dependence of the dielectric constant ( $\epsilon_1$ , upper panel) and conductivity ( $\sigma_1$ , lower panel) in magnetite at  $\nu = 12 \text{ cm}^{-1}$ . The data have been calculated from the complex reflectance (circles) of a thick sample and from the complex transmittance of a 0.05 mm thin plate (triangles). Right inset - dc-conductivity of a thick sample in full temperature range, left inset - temperature region close to the Verwey transition.

three orders of magnitude. Both transmittance and reflectance show a hysteretic behavior, characteristic for a first-order phase transition. However, the experimentally observed hysteresis extends over different temperature regimes: the hysteresis spans  $\Delta T \simeq 2 \text{ K}$  in the reflectance experiments, and is significantly less than 0.5 K in transmittance experiments. We suggest that this distinct difference probably results from the sample geometries, namely utilizing a thick sample ( $\simeq 5 \text{ mm}$ ) in the reflectance and thin sample ( $\simeq 0.05 \text{ mm}$ ) in the transmittance experiments. Except for the hysteresis region, all measurements revealed results coinciding within the experimental accuracy (Fig. 2). The effective overdetermination of the physical quantities,  $\epsilon_1$  and  $\sigma_1$ , in these experiments was necessary because of the highly unusual temperature and frequency dependence of the electrodynamic properties of magnetite (as discussed below).

Figure 2 shows the temperature dependence of the conductivity ( $\sigma_1$ ) and the dielectric constant ( $\epsilon_1$ ) of magnetite at  $\nu = 12 \text{ cm}^{-1}$ . The data have been obtained either from the complex transmittance ( $t =$

$\sqrt{T} \exp(i\phi_T)$ , triangles) or from the complex reflectance ( $r = \sqrt{R} \exp(i\phi_R)$ , circles). The conductivity reveals a sharp increase by a factor of three at the transition temperature. However, this value is substantially lower than the increase by two orders of magnitude, observed in the dc-conductivity (insets of Fig. 2). This is a direct consequence of the power-law frequency dependence of the ac-conductivity yielding orders-of-magnitude increase of the conductivity with increasing frequency.

The behavior of the dielectric constant at the Verwey transition is highly unusual. Both transmittance and reflectance experiments lead to a strong *decrease* of the dielectric constant at the metal-to-insulator transition, becoming even negative above  $T_V$ . In the classical systems revealing a metal-to-insulator transition (e.g. doped silicon) it has been observed that the dielectric constant diverges approaching the transition temperature from the insulating side [27, 37], which has been termed *dielectric catastrophe*. In agreement with this picture and using the same technique as presented here, a strong increase of the dielectric constant at the metal-insulator transition has been observed in Sr-doped  $\text{LaMnO}_3$  [38] and recently in a magnetic field-induced transition in  $\text{Pr}(\text{Ca:Sr})\text{MnO}_3$  [39]. We believe that the first-order character of the phase transition in magnetite interrupts the increase of the dielectric constant, observed at  $T < T_V$  ( $d\epsilon/dT \simeq 1 \text{ K}^{-1}$  at low frequencies). Instead, the dielectric constant of magnetite abruptly jumps to negative values at the "metallic" side of the transition.

Figure 3 shows the frequency dependence of the conductivity and dielectric constant in magnetite. Symbols at low frequencies represent the results of the transmittance experiments. Solid lines above  $30 \text{ cm}^{-1}$  have been obtained via the Kramers-Kronig analysis of the reflectance. The lower frame of Fig. 3 shows the frequency dependence of  $\sigma_1$  above and below the Verwey transition. The low-frequency conductivity in the insulating state is dominated by a power-law in frequency ( $\sigma_1 \propto \nu^s$  with  $s \sim 1.3$ ) with a temperature-dependent amplitude and a weakly temperature-dependent frequency exponent. As mentioned in the Introduction, a power-law behavior of the conductivity is a characteristic feature of hopping conduction between localized states [23, 24, 25]. Previously, the frequency exponent  $s \sim 0.7$  has been observed in magnetite at low temperatures and at kHz-frequencies [21], a value typical for the ac-conductivity in the audio-frequency range. Substantially higher values of the exponent are expected at higher frequencies: approaching the phonon-assisted-hopping regime,  $\sigma_1 \propto \nu^2$  has been predicted for low temperatures [40]. The transition to higher frequency-exponents in the microwave frequency range has been discussed recently for doped semiconductors [41]. The power-law term is generally referred to as *universal dielectric response* [22] and has been a recent matter of discussion concerning a possible universal superlinear power law with  $s \gtrsim 1$  at high frequencies [42].

The frequency dependence of the dielectric constant in magnetite is shown in the upper panel of Fig. 3.

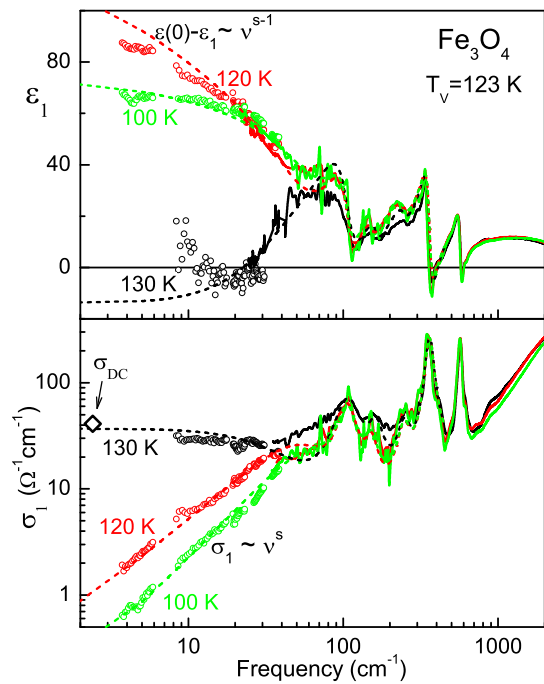


FIG. 3: (color) Frequency dependence of the conductivity ( $\sigma_1$ , lower panel) and the dielectric constant ( $\epsilon_1$ , upper panel) of magnetite above and below  $T_V \simeq 123$  K. Symbols below  $40 \text{ cm}^{-1}$  and solid lines above  $30 \text{ cm}^{-1}$  represent the experimental data, dashed lines - model calculations. Experimental data have been obtained from transmittance and phase-shift of a thin  $\text{Fe}_3\text{O}_4$  plate below  $40 \text{ cm}^{-1}$ , and via the Kramers-Kronig analysis of the reflectance of the thick sample above  $30 \text{ cm}^{-1}$ . The main contribution to the model calculations is given by the hopping term ( $\sigma^* \propto \nu^s$ , Eq. 2) below  $T_V$  and a Drude-term (Eq. 4) above  $T_V$ .

The behavior of the dielectric constant in the insulating state agrees qualitatively with the power-law of  $\sigma_1$ , i.e.  $\epsilon_1$  increases with decreasing frequency. For  $s > 1$  the low-frequency behavior can be approximated by  $\epsilon_1(0) - \epsilon_1(\nu) \propto \nu^{s-1}$ .

Dashed lines in Fig. 3 for the insulating state ( $T < T_V$ ) were obtained by fitting the experimental data to the expression

$$\sigma_1(\nu) = \sigma_{dc} + A \frac{(\nu/\nu_1)^s}{1 + (\nu/\nu_1)^4} . \quad (2)$$

Here  $\sigma_{dc}$  is the dc-conductivity and  $A$  is the amplitude of the hopping process. Compared to the conventional form of this response [22, 23, 24, 25, 42], we introduced an additional high-frequency cutoff  $[1 + (\nu/\nu_1)^4]$ . The cutoff frequency  $\nu_1$  only weakly influences the conductivity in the low-frequency range but prevents the divergence of the spectral weight of  $\sigma_1 \propto \nu^s$  at high frequencies.

The analytical expression for the dielectric constant has been obtained by applying the Kramers-Kronig transformation [43] to Eq. (2) which gives the following

TABLE I: Parameters of the THz-frequency excitations in magnetite close to the Verwey transition which correspond to Eqs. (2,3,4). The changes in conductivity can be well described assuming the transformation of the hopping term Eq. (2) into the Drude-term Eq. (4) with a high mobility of the quasi-free carriers.

T (K)	$\nu_1 (\text{cm}^{-1})$	s	$A (\Omega^{-1} \text{cm}^{-1})$
100	70	1.5	39
120	60	1.2	44
T (K)	$1/2\pi\tau (\text{cm}^{-1})$	$\sigma_{dc} (\Omega^{-1} \text{cm}^{-1})$	
130	40	37	

analytical expression for the dielectric constant:

$$\epsilon_1(\nu) = \frac{\sigma_1(\nu) - \sigma_{dc}}{2\pi\nu\epsilon_0} \left\{ \tan(s\pi/2) - \frac{(\nu/\nu_1)^{1-s}}{\cos(s\pi/2)} \left[ \sin[(s+1)\frac{\pi}{4}] + \left(\frac{\nu}{\nu_1}\right)^2 \cos[(s+1)\frac{\pi}{4}] \right] \right\} \quad (3)$$

This expression is valid both for  $s < 1$  and for  $s > 1$ .

To take into account the phononic and high-frequency electronic contributions, the sum of 6 Lorentzians has been added to expressions Eq.(2) and Eq.(3). Five Lorentzians at frequencies of 106, 152, 247, 361, and  $574 \text{ cm}^{-1}$  represent phonon contributions. Additional over-damped oscillator at  $4270 \text{ cm}^{-1}$  ( $0.53 \text{ eV}$ ) approximates the first excitation of the electronic origin. The given characteristic frequencies agrees well with the published data [13, 14, 15]. In order to simplify the analysis of the THz conductivity and obtain the essential physics of the problem, the contributions from the Lorentzians were fixed for all three temperatures in Fig. 3. The parameters obtained from simultaneous fitting of the conductivity and dielectric constant are given in Table I.

A remarkable feature of the parameters for the low-temperature insulating phase in Table I is the low value of the cutoff frequency  $\nu_1$ . Indeed, a qualitative examination of the conductivity frame of Fig. 3 reveals that the hopping process  $\sigma_1 \propto \nu^s$  and the low-frequency edge of the electronic excitation ( $\nu > 1000 \text{ cm}^{-1}$ ) are well separated in energy. This indicates that the cutoff frequency of the hopping must be in the range  $\sim 100 \text{ cm}^{-1}$ , in agreement with the fits. This result is rather surprising and suggests that the low-temperature conductivity is governed by phonons.

In contrast to the gradual variation of  $\epsilon_1(\omega, T)$  and  $\sigma_1(\omega, T)$  at low temperatures, dramatic changes are observed at the Verwey transition. At low frequencies the conductivity increases by more than one order-of-magnitude. This increase is substantially smaller than a change of two orders-of-magnitude in dc-conductivity (see insets of Fig. 2). This difference is the result of a power-law frequency dependence of the conductivity

in the insulating state. As a consequence, for frequencies close to  $35\text{ cm}^{-1}$  we observe almost *no conductivity change* at  $T_V$ . This observation has been verified in a separate temperature-dependent experiment at  $\nu = 35\text{ cm}^{-1}$  (not shown).

As discussed above, the decrease of the dielectric constant at the transition to the conducting state is not expected within the scope of a conventional metal-insulator transition scenario. In order to find an explanation to this experimentally-observed behavior, we mention that a negative dielectric constant naturally follows by assuming a Drude-response of quasi-free carriers,

$$\sigma_{\text{DR}}^* = \sigma_{dc}/(1 - i2\pi\nu\tau), \quad (4)$$

where  $\sigma_{dc}$  and  $1/2\pi\tau$  are dc-conductivity and scattering rate, respectively. In addition to the negative changes in  $\varepsilon_1$ , the conductivity in the metallic state shows a slight downward curvature in the frequency dependence (lower panel of Fig. 3). This provides a further argument to include a Drude-term to the model. Indeed, the simplest way to reproduce the experimental changes between 120 and 130 K is just to *replace* the hopping term (Eq. 2,3) by the Drude term. For the second sample of magnetite with  $T_V \simeq 116\text{ K}$  a qualitatively similar behavior has been observed and the absolute values of the parameters agreed within  $\sim 20\%$ . We believe that this variation partly corresponds to the difference in the conductivities of the samples.

The low value of the scattering rate, as observed in the present experiments, corresponds to a high carriers mobility of  $\mu = e\tau/m \simeq 10^3\text{ cm}^2/Vs$  (assuming  $m$  being the free electron mass) and correlates well with the high quality of our magnetite single crystals. Due to the low characteristic frequency of the coherent (itinerant) process, its spectral weight

$$S = \frac{2}{\pi} \int_0^{\infty} \sigma_{1,DR}(\omega) d\omega = \sigma_{dc}/\tau \quad (5)$$

is small compared to the full number of carriers. Taking as an estimate of the total spectral weight the concentration of  $\text{Fe}^{2+}$  ions [29], only about  $2 \cdot 10^{-4}$  of the theoretically-available carriers participate in the coherent process. We recall further, that within the rough estimate the spectral weight of thermally-activated quasi-free carriers in a semiconductor can be written as

$$S = \frac{ne^2}{m_{eff}} \exp\left(-\frac{\Delta_m}{k_B T}\right), \quad (6)$$

where  $n$ ,  $e$  and  $m_{eff}$  are concentration, charge and effective mass of the charge carriers, respectively. In this expression the effective concentration of charge carriers is temperature-activated and is governed by an energy gap  $\Delta_m$ . The estimate of the effective mass  $m_{eff} \simeq 10^2 m$

has been obtained from the infrared conductivity [14] and from the small-polaron analysis of photoemission of the same sample [11]. With this estimate for  $m_{eff}$  the observed small spectral weight of the Drude-process corresponds to  $\Delta_m \simeq 40\text{ meV}$ , which correlates with a weakly-activated dc-conductivity just above  $T_V$  (right inset in Fig. 2). Within the same picture, the Verwey transition in magnetite corresponds just to an increase of the characteristic activation energy at the insulating side of the transition. The drop of dc-conductivity at the transition can be ascribed to a gap change from  $\Delta_m \simeq 40\text{ meV}$  (conducting state) to  $\Delta_i \simeq 90\text{ meV}$  (insulating state). This new value of the energy gap agrees with the activation energy of dc-conductivity [18, 19, 20], thermoelectric power [12], and with the gap values obtained in photoemission experiments [9, 10, 11]. The presented description implies the interpretation of Verwey transition as an insulator-semiconductor transition with a change in activation energy induced by crystal structure or by electronic configuration.

#### IV. CONCLUSIONS

Terahertz and infrared conductivity in magnetite has been obtained on both sides of Verwey metal-to-insulator transition. Two orders-of-magnitude change in dc-conductivity halves at millimeter frequencies and even disappears for  $\nu \gtrsim 30\text{ cm}^{-1}$ . In the far-infrared range the effect of the transition remains solely in changing the dielectric constant ( $\varepsilon_1$ ) of magnetite. The change of  $\varepsilon_1$  during the transition into the conducting state is negative, which is in surprising contrast to an expected (positive) divergence of the dielectric constant at a metal-insulator transition. Within the simple model-analysis the conductivity mechanism switches between hopping of localized carries below  $T_V$  and itinerant motion above  $T_V$ . These results evidence the formation of the coherent state on the metallic side of the Verwey transition with high mobility of the charge carriers. Together with the recent photoemission data on the same samples the interpretation of the Verwey transition as an insulator-semiconductor transition is suggested.

#### V. ACKNOWLEDGEMENTS

The stimulating discussion with P. Lunkenheimer, L. V. Gasparov and I. Leonov is gratefully acknowledged. We thank A. A. Volkov, P. Pfalzer and A. Pimenova for help in sample preparation and S. Klimm for the measurement of the dc-conductivity. This work was supported by BMBF (13N6917/0 - EKM) and by DFG (SFB484 - Augsburg).

- 
- [1] E. J. W. Verwey and P. W. Haayman, *Physica* (Amsterdam) **8**, 979 (1941); E. J. W. Verwey, P. W. Haayman, and F. C. Romeijn, *J. Chem. Phys.* **15**, 181 (1947).
- [2] F. Walz, *J. Phys.: Cond. Matter* **14**, R285 (2002).
- [3] J. García and G. Subías, *J. Phys.: Cond. Matter* **16** R145 (2004).
- [4] G. Subías, J. García, J. Blasco, M. G. Proietti, H. Renevier, and M. C. Sánchez, *Phys. Rev. Lett.* **93**, 156408 (2004); J. García, G. Subías, M. G. Proietti, J. Blasco, H. Renevier, J. L. Hodeau, and Y. Joly, *Phys. Rev. B* **63**, 054110 (2001).
- [5] I. Leonov, A. N. Yaresko, V. N. Antonov, M. A. Korotin, and V. I. Anisimov, *Phys. Rev. Lett.* **93**, 146404 (2004).
- [6] M. Iizumi, T. F. Koetzle, G. Shirane, S. Chikazumi, M. Matsui and S. Todo, *Acta Cryst. B* **38**, 2121 (1982).
- [7] J. M. Zuo, J. C. H. Spence, and W. Petuskey, *Phys. Rev. B* **42**, 8451 (1990).
- [8] J. P. Wright, J. P. Attfield, and P. G. Radaelli, *Phys. Rev. Lett.* **87**, 266401 (2001); *Phys. Rev. B* **66**, 214422 (2002).
- [9] A. Chainani, T. Yokoya, T. Morimoto, T. Takahashi, and S. Todo, *Phys. Rev. B* **51**, 17976 (1995).
- [10] J.-H. Park, L. H. Tjeng, J. W. Allen, P. Metcalf, and C. T. Chen, *Phys. Rev. B* **55**, 12813 (1997).
- [11] D. Schrupp, M. Sing, M. Tsunekawa, H. Fujiwara, S. Kasai, A. Sekiyama, S. Suga, T. Muro, V.A.M. Brabers, and R. Claessen, cond-mat/0405623.
- [12] A. J. M. Kuipers and V. A. M. Brabers, *Phys. Rev. B* **14**, 1401 (1976).
- [13] S. K. Park, T. Ishikawa, and Y. Tokura, *Phys. Rev. B* **58**, 3717 (1998).
- [14] L. V. Gasparov, D. B. Tanner, D. B. Romero, H. Berger, G. Margaritondo, and L. Forró, *Phys. Rev. B* **62**, 7939 (2000).
- [15] L. Degiorgi, P. Wachter, and D. Ihle, *Phys. Rev. B* **35**, 9259 (1987); A. Schlegel, S. F. Alvarado, and P. Wachter, *J. Phys. C* **12**, 1157 (1979).
- [16] D. Ihle and B. Lorenz, *J. Phys. C: Sol. State Phys.* **18**, L647 (1985); *ibid.* **19**, 5239 (1986).
- [17] C. Presura, M. Popinciuc, P. H. M. van Loosdrecht, D. van der Marel, M. Mostovoy, T. Yamauchi, and Y. Ueda, *Phys. Rev. Lett.* **90**, 026402 (2003).
- [18] B. A. Calhoun, *Phys. Rev.* **94**, 1577 (1954).
- [19] M. Matsui, S. Todo and S. Chikazumi, *J. Phys. Soc. Jpn.* **42**, 1517 (1977).
- [20] A. J. M. Kuipers and V. A. M. Brabers, *Phys. Rev. B* **20**, 594 (1979).
- [21] Y. Akishige, T. Fukatsu, M. Kobayashi, and E. Sawaguchi, *J. Phys. Soc. Jpn.* **54**, 2323 (1985); M. Kobayashi, Y. Akishige, and E. Sawaguchi, *ibid.* **55**, 4044 (1986).
- [22] A. K. Jonscher, *Dielectric Relaxation In Solids* (Chelsea Dielectrics, London, 1983).
- [23] A. R. Long, *Adv. Phys.* **31**, 553 (1982).
- [24] S. R. Elliott, *Sol. St. Ionics* **27**, 131 (1988).
- [25] J. C. Dyre and T. B. Schrøder, *Rev. Mod. Phys.* **72**, 873 (2000).
- [26] A. F. Ioffe and A. R. Regel, *Progr. Semicond.* **4**, 237 (1960).
- [27] N. F. Mott, *Metal-Insulator Transitions* (Taylor & Francis, London, 1990), p. 35.
- [28] J. Honig, in *Metallic and Non-Metallic States of Matter*, edited by P. P. Edwards and C. N. Rao (Taylor & Francis, London, 1985), p. 226.
- [29] N. Tsuda, K. Nasu, A. Yanase, and K. Siratori, *Electronic Conduction in Oxides* (Springer, Berlin, 1991) p. 207.
- [30] M. Imada, A. Fujimori, and Y. Tokura, *Rev. Mod. Phys.* **70**, 1039 (1998).
- [31] V.A.M. Brabers, *J. Cryst. Growth* **8**, 26 (1971).
- [32] V.A.M. Brabers F. Walz and H. Kronmüller, *Phys. Rev. B* **58**, 14163 (1998).
- [33] G. V. Kozlov and A. A. Volkov in *Millimeter and Submillimeter Wave Spectroscopy of Solids*, edited by G. Grüner (Springer, Berlin, 1998), p.51; A. A. Volkov, Yu. G. Goncharov, G. V. Kozlov, S. P. Lebedev, and A. M. Prochorov, *Infrared Phys.* **25**, 369 (1985).
- [34] O. S. Heavens, *Optical properties of thin solid films* (Dover Publ., New York, 1991).
- [35] M. Born and E. Wolf, *Principles of optics* (Pergamon, Oxford, 1986).
- [36] A. Pimenov, A. Loidl, and S. I. Krasnosvobodtsev, *Phys. Rev. B* **65**, 172502 (2002).
- [37] H. F. Hess, K. DeConde, T. F. Rosenbaum, and G. A. Thomas, *Phys. Rev. B* **25**, 5578 (1982); M. Capizzi, G. A. Thomas, F. DeRosa, R. N. Bhatt, and T. M. Rice, *Phys. Rev. Lett.* **44**, 1019 (1980).
- [38] A. Pimenov, C. Hartinger, A. Loidl, A. A. Mukhin, V. Yu. Ivanov, and A. M. Balbashov, *Phys. Rev. B* **59**, 12419 (1999).
- [39] D. Ivannikov *et al.*, unpublished.
- [40] N. F. Mott and E. A. Davis, *Electronic processes in non-crystalline materials*, (Clarendon Press, Oxford, 1979).
- [41] E. Helgren, N. P. Armitage, and G. Grüner, *Phys. Rev. B* **69**, 014201 (2004); M. Lee and M. L. Stutzmann, *Phys. Rev. Lett.* **87**, 056402 (2001).
- [42] P. Lunkenheimer and A. Loidl, *Phys. Rev. Lett.* **91**, 207601 (2003).
- [43] F. Wooten, *Optical Properties of Solids* (Acad. Press, NY, 1972) p.173.